A photographic method for drop characterization in agricultural sprinklers

by

Salvador, R.[1], Bautista-Capetillo, C.[2],

Burguete, J.[1], Zapata, N.[1], Serreta, A.[3] Playán, E.[1]

ABSTRACT

The characterization of drops resulting from impact sprinkler irrigation has been addressed by a number of techniques. In this paper, a new technique based on low-speed photography (1/100 s) is presented and validated. The technique permits to directly measure drop diameter, velocity and angle. The photographic technique was applied to the characterization of drops resulting from an isolated sprinkler equipped with a 4.8 mm nozzle and operating at a pressure of 200 kPa. Sprinkler performance was characterized from photographs of 1,464 drops taken at distances ranging from 1.5 to 12.5 m. It was possible to analyze separately the drops emitted by the main jet and those emitted by the impact arm. The proposed technique does not require specific equipment, although it is labour intensive.

Keywords: impact sprinkler, drop, diameter, velocity, angle, photography, low-speed.

[1] Dept. Soil and Water, Aula Dei Experimental Station, CSIC. P.O. Box. 202, 50080 Zaragoza, Spain. rsalvador@eead.csic.es, jburguete@eead.csic.es, vzapata@eead.csic.es, enrique.playan@eead.csic.es

[2] Dept. Planeación de Recursos Hidráulicos, Universidad Autónoma de Zacatecas. Avda. Ramón López Velarde, 801. Zacatecas, Zacatecas, México. baucap@uaz.edu.mx

[3] Escuela Politécnica Superior de Huesca, Universidad de Zaragoza. Ctra. de Cuarte, s/n, 22071. Huesca, Spain. serreta@unizar.es.

INTRODUCTION

The characterization of drops resulting from impact sprinkler irrigation typically implies the determination of their diameter as they approach the soil surface. Drop characterization has been used for different purposes related to irrigation management, such as evaporation losses, soil conservation and irrigation simulation. Evaporation losses have often been empirically correlated with wind speed (Edling 1985; Trimer 1987; Keller and Bliesner 1990; Tarjuelo et al. 2000; Playán et al. 2005). Wind speed has been found to affect fine drops much more than large drops (Fukui et al. 1980; Thompson et al. 1986, De Lima et al. 1994; De Lima et al. 2002). Lorenzini (2006) presented a theoretical analysis of water droplet evaporation, and stressed the importance of air friction and air temperature on the process. Regarding soil conservation, drop kinetic energy results in soil surface sealing, compaction and erosion (Bedaiwy 2008). This energy is directly related to drop diameter and velocity (Kincaid 1996). In kinetic energy analyses of sprinkler irrigation, drop velocity was estimated using simulation models (Kincaid 1996). When it comes to simulating sprinkler irrigation, the distribution of drop diameters is a primary input. An adequate characterization of this variable is required to estimate the differences in performance resulting from different irrigation equipments, operating conditions or changes in the environment (particularly wind speed). Ballistic sprinkler simulation models (Carrión et al. 2001; Playán et al. 2006) require this information to estimate the landing point and terminal velocity of drops resulting from a certain irrigation event. Procedures have been developed to estimate drop diameter distribution at the nozzle from the sprinkler application pattern using inverse simulation techniques (Montero et al. 2001; Playán et al. 2006). Following these techniques, drop distributions can be identified that reproduce observed application patterns.

As a consequence of these irrigation management and simulation needs, irrigation drop characterization has been a traditional field of research. Different techniques have been developed since the end of the 19th Century (Wiesner 1895). The evolution of drop characterization techniques as related to natural or irrigation precipitation has been reported by a number of authors (Cruvinel et al. 1996; Cruvinel et al. 1999; Salles et al. 1999; Sudheer and Panda 2000; Montero et al. 2003). A succinct discussion of the methods reported in these papers follows:

- **Stain method**. It is based on the measurement of the stain created by a drop when impacting on an absorbing surface. Since stain and drop diameters are correlated, stain diameters can be used to estimate drop diameters (Magarvey 1956).
- **Flour method**. Drops impacting on a thin layer of flour create pellets whose mass or diameter is statistically related to drop diameter (Kohl and DeBoer 1984)
- **Oil immersion method**. Based on the fact that water droplets can get trapped in a fluid with adequate density. Drops are then observed with appropriate optical equipment to measure their diameter (Eigel and Moore 1983)
- **Momentum method**. Includes a variety of techniques (mostly applied to natural precipitation) based on the use of pressure transducers to estimate the kinetic properties of sets of drops (Joss and Waldvogel 1967).
- **Photographic method**. The methodology is based on high-speed photographs of drops in an irrigation jet. The technique first focused on photographing raindrops (Jones 1956). Recently, photographs have been used to estimate drop diameter through digital techniques (Sudheer and Panda 2000).
- **Optical methods**. In the last decade of the 20th Century, two types of optical methods were applied to measure drop diameter. The first one is based on the analysis of the deviation of a laser flow as it passes through drops of different

characteristics (Kincaid et al. 1996). The second one, the optical disdrometer, measures the attenuation of a luminous flow (Hauser et al. 1984; Montero et al. 2003). Both methods provide automated estimates of drop diameter in a set of drops.

Optical methods count on the advantage of being fully automated in data collection, thus permitting fast, repeatable drop characterization. These methods have however specific sources of errors, such as those induced by side-passing drops and overlapping drops. Recently, (Burguete et al. 2007) presented a simulation study characterizing the relevance of these errors under a number of experimental conditions, and proposed a statistical method to reject erroneous drops. Burguete et al. (2007) theoretically analysed the use of the disdrometer to estimate drop velocity from drop time of passage, and found it subjected to large experimental errors.

The need for an alternative, simple method for evaluating the characteristics of sets of drops motivated the search for a direct drop characterization method able to provide information on at least drop diameter and velocity. Recent developments in digital photography oriented the search towards a photographic method which could be used to obtain data sets adequate for detail analysis of sprinkler irrigation problems. Such a method stands as an attractive alternative, since it does not require specific equipment.

In this paper a new photographic technique is presented, validated and tested. The technique permits to measure the diameter, velocity and angle (in a vertical plane containing the drop trajectory) of each drop. The proposed technique is based on low-speed photography rather than on high-speed photography. Under low-speed conditions, drops are photographed as traces of the drop trajectory, thus permitting determination of the three abovementioned variables. Under high-speed conditions, it is only possible to determine drop diameter, since drops are visualized as spheres. The results of the proposed low-speed photography technique were applied in this paper to characterize water application resulting from an isolated impact sprinkler.

MATERIALS AND METHODS

Basic experimental set up

A VYR35 impact sprinkler (VYRSA, Burgos, Spain) was used in all experiments. This model is commonly used in solid-set systems in Spain. The sprinkler was equipped with a 4.8 mm nozzle (including a straightening vane). An isolated sprinkler was installed at an elevation of 2.15 m and operated at a nozzle pressure of 200 kPa. The sprinkler revolution time was 27.5 s. A volumetric water meter was used to estimate sprinkler discharge. The experimental runs were performed at the CITA farm located in Montañana, Zaragoza (Spain). A plot was chosen which was protected from the prevailing winds by a windbreak. Experiments were performed in periods of inappreciable wind.

Characterization of the radial application pattern

In order to achieve this objective, 28 pluviometers were installed on the experimental plot along a sprinkler radius, covering distances from 1.5 m to 14.0 m, with 0.5 m interval. The pluviometer dimensions were in compliance with the ISO 15886-3 norm. The irrigation test lasted for two hours, during which 2.495 m^3 of irrigation water were applied (average discharge of 0.347 L s^{-1}).

Preliminary photographic experiments for drop characterization

Using a relatively low shutter speed, drops are represented in the photographs as cylinders, thus permitting the identification of drop diameter and length of run (by comparison with a photographed reference ruler), and vertical angle. Drop velocity can be derived from the length of run and the shutter speed.

Preliminary experiments were performed to identify optimum camera operation conditions for outdoor drop identification. The camera zoom was always set at 70 mm. After trying several background screen colours, black was chosen as the best option for drop characterization. In a second step, different shutter speeds (100, 125 and 160) and diaphragm openings (from F4.5 to F29) were tested. The chosen combination was a shutter speed of 100 (1/100 s) and F11. These camera adjustments resulted in sharp drop cylinder images.

In all subsequent experiments, the camera and the screen were installed as depicted in Fig. 1, to allow for drops to fall between them. The screen was built to suit the needs of the experiment. It consisted of a plastic rectangle of 0.30 x 0.40 m covered with a black cloth to prevent drops on the plastic material from shining and thus disturbing the characterization of falling drops. A reflecting metallic lateral was mounted on the side of the screen (opposite to the sun) to increase the drop brightness by duplicating the source of light (sun and reflector). The screen was installed at a distance of 1.00 m from the camera objective. The reference ruler was installed on the screen, at a distance of 0.25 m from it (0.75 m from the camera objective). The camera was manually focused on the reference ruler.

Subsequently, tests were performed to determine how many photographs could be taken when shooting in continuous mode and what the speed of picture taking was. These values depend of the selected photo quality. Quality “L” (3,872 by 2,592 pixels) was selected because this was the highest available image resolution in JPEG format, and the picture taking speed was adequate (2.9 photos per second). The combination of photo quality, zoom regulation and distance to the target resulted in a density of 14-15 pixels mm^{-1}. As a consequence, drops of 0.5 mm would have a diameter of about 7 pixels, while drops of 5 mm would have a diameter of 70-75 pixels. Regarding the length of the drop trace (cylinder height), it fluctuated between 130 and 1,050 pixels, depending on drop velocity.

Validation of the proposed photographic method

An experiment was performed to validate the main features of the method. Drops were modelled using metallic spheres of known diameter and physically determined velocity. A digital micrometer was used to determine an average diameter of 4.49 mm, and a coefficient of variation in diameter of 0.69 %. The experimental density of the lead-based spheres was 11.2 Mg m^{-3}. A set of spheres was released from an elevation of 0.55 m over the 0 mark on the reference ruler. Photographs were used to determine sphere diameter and velocity. Due to the short trajectory of the spheres and the high metal density, acceleration was relevant when spheres were photographed. Consequently, for each sphere, the elevation from the release point to the centre of the photographed trajectory was determined. In order to test the photographic depth-of field and to estimate the related errors, spheres were released from five different points, differing in distance to the camera objective. The first release point was just above the reference ruler. The remaining four points were closer to the camera objective by 0.02, 0.04, 0.06 and 0.08 m, respectively. In all five cases, the camera objective was focused to the reference ruler.

Diameter validation consisted on comparing micrometric measurements and photographic estimates of sphere diameter at different distances from the reference ruler. Regarding sphere velocity, the ballistic theory applied to drop movement was analysed (Fukui et al. 1980; Seginer et al. 1991). Under the experimental conditions the drag force was orders of magnitude smaller than the sphere weigh. As a consequence, sphere movement could be approximated by the free fall equation:

$$V = \sqrt{2\, g\, h} \qquad [1]$$

Where V is vertical velocity, g is the acceleration of gravity, and h is elevation from the release point.

Experimental runs for drop characterization: field procedures

Field experiments for drop characterization began at the experimental plot with the isolated sprinkler (Fig. 1), in sessions lasting between one and two hours. Nozzle pressure was controlled with a manometer and adjusted to 200 kPa. A radial line was marked on the soil extending from the sprinkler to the last observation point. The line was marked in every experimental period so that it formed a horizontal angle of about 5º with the sun. Observation points for drop photography were marked on the line at distances of 1.5, 3.0, 4.5, 6.0, 7.5, 9.0, 10.5 and 12.5 m from the sprinkler. While the interval between observation points was usually 1.5 m, between the last two observation points the interval was 2.0 m. This interval was chosen so that photographs could be taken at 12.5 m, the last distance from the sprinkler at which drops could be appreciated at the camera elevation (0.80 m). It was judged interesting to photograph the drops reaching the largest distances from the sprinkler.

At each observation point, the camera and the screen were installed (Fig. 1). When the sprinkler jet approached the measurement line, the camera shooting was activated in continuous mode. Shooting stopped when drops could not be appreciated. Consequently, the number of photographs was different in each experimental run. In fact, this number depended on the time the jet stayed over the observation point (in turn dependent on distance to the sprinkler). This procedure was repeated between three and ten times at each observation point, depending on the local drop density (number of drops per unit photographed area). Drop density was very high near the sprinkler, while at the distal areas a large number of photographs were required to obtain a representative sample of the local drop population.

Although the sprinkler nozzle produces one compact jet of drops, the sprinkler impact arm takes some of its water to create a new, small jet at a certain horizontal angle. At distances of 6.0 and 7.5 m from the sprinkler, the time lag between the drops coming from the impact arm and those coming from the main jet was long enough to photograph both sources of drops separately. At smaller distances no distinction could be made, while impact arm drops were not observed at distances exceeding 7.5 m.

Experimental runs for drop characterization: office procedures

At every observation point a large number of photographs were taken. Some of them showed drops of adequate quality. These photographs were selected for further analysis using Microsoft Picture Manager®. The values of brightness, contrast and semitone were fixed at 60, 85 and 100 %, respectively, for all images.

The GIMP2© software (University of California, Berkeley, USA) was used for drop analysis. Drops adequately focused (located near the vertical plane containing the reference ruler) were numbered for future reference. Due to the available image resolution, drops not reaching 0.3 mm in diameter were discarded since it was impossible to assess if they were focused. The following step was to measure drop length, angle respect to the horizontal (setting the 0º at the line starting at the camera objective and perpendicularly intersecting the sprinkler riser), and drop diameter (correcting the number of horizontal pixels with the drop angle). If for a given drop the complete cylinder was not represented in the photograph, drop velocity was not measured. However, the drop diameter and angle were added to the drop database. All values were initially registered in pixels and transformed to mm using the pixel mm^{-1} ratio obtained from the analysis of the image of the reference ruler. Histograms of the three analyzed variables were produced at each observation distance.

Drop diameter was combined with the sprinkler application pattern to estimate cumulative applied volume at a certain distance from the sprinkler.

RESULTS AND DISCUSSION

Characterization of the radial application pattern

The first step for sprinkler characterization was to obtain the radial application pattern using pluviometer data (Figure 2). The resulting pattern is characteristic of impact sprinklers operating at low pressure. It shows low precipitation values (as low as 1.2 mm h^{-1}) at intermediate distances (5-7 m from the sprinkler), and maximum values near the end of the irrigated area. The minimum recorded precipitation was 0.2 mm h^{-1} at 14.0 m from the sprinkler, while the maximum precipitation was 2.8 mm h^{-1} at 11.0 m. The average precipitation along the irrigated radius was 1.6 mm h^{-1}.

Validation of the proposed photographic method

Photographs taken at distances between the spheres and the vertical plane containing the reference ruler of 0.06 and 0.08 m were out of focus and could not be evaluated. As a consequence, the proposed method characterizes drops located in a range of ± 0.04 m from the focus point (the reference ruler). A total of 43 photographs containing 138 trajectories of the validation metallic spheres (corresponding to the distances to the reference ruler of 0.00, 0.02 and 0.04 m) were evaluated.

The average measured sphere diameters were 4.47, 4.59 and 4.60 mm, for distances of 0.00, 0.02 and 0.04 m, with respective coefficients of variation of 2.01, 2.74 and 3.13 %. The increase in diameter with decreased distance to the target reflects the error derived from spheres which appear larger than they are because they are closer to the camera objective. In the worst case, spheres with a real diameter of 4.49 mm resulted in estimated diameters of 4.60 mm. As a consequence, the proposed method results in a maximum average error of ± 2.45 % at a distance of 0.04 m from the reference ruler. Under a random fall of spheres, the errors produced on both sides of the reference ruler cancel, and the average error can be approximated by the average diameter error at a distance of 0.00 m (-0.45 %). These maximum and average error figures are moderate, and can be compared to the manufacturing coefficient of variation of the spheres (±0.69 %).

Regarding drop velocity, the average simulated velocity was 3.26 m s^{-1}. The average measured velocities were 3.27, 3.28 and 3.22 m s^{-1} at 0.00, 0.02 and 0.04 m from the reference ruler, respectively. The expected average error corresponds to the error at 0.00 m (0.31 %), while the maximum average error was 1.23 % at a distance of 0.04 m from the ruler. In the case of sphere velocity, however, photographic measurements were compared to simulation results, not to velocity measurements.

Drop angle was not validated, due to the physical nature of its measurement procedure and its independence from the distance to the reference ruler.

The errors in diameter and velocity resulting from the spheres being closer or further to the camera objective than the reference ruler cancel out when average values are produced. These errors result in modified distributions of diameters and velocities. The maximum errors have been bounded in the reported experiment (±2.45 % for diameter and ±1.23 % for velocity). These error bounds must be taken into consideration when analysing the results presented in this paper, but the magnitude of the errors does not compromise the validity of the results.

Basic drop statistics

A large number of photographs (about 600) were taken. Only 184 of them contained valid drops. The rest of the photographs were taken before or after the jet passage, or contained very few, unfocused drops. The total number of valid drops was 1,464. Table 1 presents basic statistics (mean, minimum and maximum) of the number of drops and the analyzed variables (arithmetic diameter, volumetric diameter, velocity and angle) as a function of the distance to the sprinkler. The number of drops ranged from

61 at 12.5 m to 354 at 1.5 m. Average drop diameter increased with distance, with a minimum of 0.6 mm at 1.5 m, and a maximum of 3.3 mm at 12.5 m. The volumetric diameter followed a similar pattern, increasing from 0.7 mm at 1.5 m to 4.1 mm at 12.5 m. Drop velocity also increased with distance, ranging from 1.9 m s^{-1} by the sprinkler to 5.6 m s^{-1} at the limit of irrigated area. Average angle values resulted quite variable, and it was not possible to appreciate a relationship with distance to the sprinkler. In the proximal region the angle was sometimes larger than 90º. This can be attributed to the fact that the experimental setup was located outdoor. As a consequence, turbulences could have distorted drop angle, particularly for small drop diameters. An extended version of Table 1, individualizing each drop within each distance from the sprinkler, can be downloaded from www.eead.csic.es/drops.

Figure 3 presents photographs of drops #204, #646 and #1,456. At the bottom of each picture, information is provided on the distance to the sprinkler (D), drop diameter (∅), drop velocity (V) and drop angle (â). To ease visualization, images are presented in different scales. The photographs depict drops as transparent cylinders, and permit accurate, direct determination of their size, even for the smallest diameters. The quality of the photographs permits to obtain the information required to characterize the sprinkler application pattern at any distance. Comparison between the three pictures illustrates the effect of the distance to the sprinkler on drop diameter (increase) and velocity (increase).

Drop diameter vs. distance

Drop diameter distribution histograms are presented in Fig. 4 for all distances to the sprinkler. As the distance to sprinkler increases, the frequency of large drops increases. The smooth transition observed for distances up to 9.0 m becomes abrupt between distances of 9.0 and 10.5 m. These differences could be attributed to the fact that drops landing at distances under 10.5 m from the sprinkler can either be emitted from the nozzle or separate from the jet along its trajectory. This fact could explain the presence of drops with diameters under 1 mm (about 40 % at 9.0 m), which completely disappear at a distance of 10.5 m. From 10.5 m on, all drops seem to result from the disintegration of the jet, and the modal diameters are in the interval 2-4 mm. This hypothesis was presented by Von Bernuth and Giley (1984) and Seginer et al. (1991). Montero et al. (2003) reported similar results when analyzing drop diameter measurements performed with an optical disdrometer. The uncertainties associated to disdrometer measurements, evidenced by Burguete et al. (2007) raised some concern about the quantitative importance of these small drops. Photographic data confirm the relevance of small drops at large distances from the sprinkler, and pose additional concerns about the adequacy of sprinkler irrigation ballistic theory, specifically about the hypothesis stating that all drops are created at the nozzle.

At distances from the sprinkler of 6.0 and 7.5 m, part of the drops were identified as being created by the oscillations of the impact arm, while the rest of the drops were attributed to the main jet. In Figs. 4, 5 and 6, the frequency of these drops is presented in black columns. Since impact arm and main jet drops were separated in the Figure, it could be observed that impact arm drops were larger than main jet drops at each distance.

Drops under 1 mm constituted the most frequent class for distances up to 7.5 m. The observation distance with the largest frequency of small drops was 1.5 m (98 %). From this distance on, the frequency of small drops decreased as the frequency of large drops increased. The largest diameters (larger than 4 mm) were only present at distances of 10.5 and 12.5 m, and showed frequencies of about 15 %. At a distance of 12.5 m, drops exceeding 5 mm in diameter were more frequent than at 10.5 m, the other distance where they were found.

Drop velocity vs. distance

Drop velocity resulted more variable than drop diameter for each considered distance. Figure 5 presents the frequency of drop velocity at the observation points. An increase of velocity with distance can be appreciated in the Figure, where three patterns can be observed: 1) Up to a distance of 6 m, velocities were low-medium (up to 5 m s^{-1}). Low velocities (< 3.0 m s^{-1}) prevailed at 1.5 m and at 3.0 m, accommodating about 95 % of the drops in both cases. At distances 4.5 m and 6.0 m, a gradual increase of velocity with distance was evidenced; 2) Between 7.5 and 9.0 m, a nearly homogeneous distribution of velocity could be observed in the range 0-6 m s^{-1}; 3) Finally, for distances 10.5 and 12.5 m, velocities were in the medium-high range (4-6 m s^{-1}). Drops emerging from the impact arm (depicted in black in Fig. 5) showed higher velocities than the rest of drops at the same distances. This can be attributed to the abovementioned differences in diameter.

Drop angle vs. distance

Drop angle showed the widest fluctuations among the three analyzed variables (Fig. 6). While wind speed was inappreciable during the experiments, turbulences seem to have occasionally influenced drop angle, particularly for the smallest drops. Angles slightly under 90º should be expected, as characteristic of drops reaching the soil surface with a certain component of velocity in the *x* direction. Although most drops show angles in the range 65-95º, the frequency of drops falling with angles in the >95º range is relevant at some distances. The drop diameter pattern (particularly the frequency of small drops) can contribute to explain the variability in drop angle. For distances of 9.0 m and beyond, drops with angles exceeding 85º were practically non-existent (1 % at 9.0 and 10.5 m; 0 % at 12.5 m). Drops landing at these distances were comparatively large and therefore less likely to be affected by turbulences. Drops with angle >85º had a frequency of 96 % at a distance of 1.5 m. This result can be related to the small drop diameter (< 1 mm in 98% of the drops). Drops with angle >85º also showed a large frequency at 7.5 m (67 %). In the remaining distances, this range of angles was symbolic. Drops with angle 75-85º appeared in very variable frequencies. Drop angles <75º prevailed at larger distances, with frequencies of 83% at 9.0 m, 75 % at 10.5 m and 98 % at 12.5 m. In the remaining distances, frequencies fluctuated without a clear trend. Drops emerging from the impact arm had lower angles than the rest of the drops at the same distances, with the most frequent class being <65º. While this can be partially attributed to their comparatively large diameter, the action of the arm seems to modify the vertical drop trajectory respect to drops of similar diameter resulting from the main jet.

Cumulative drop frequency and volume

Cumulative drop frequency and volume *vs.* drop diameter are presented in Fig. 7 (subfigures 1 and 2, respectively). The graphs show one cumulative line for each observation distance to the sprinkler. Cumulative frequency lines approach 100 % at smaller drop diameters than cumulative volume. This indicates than although the number of large drops is low, their volume contribution is quite large. The cumulative lines corresponding to distances 10.5 and 12.5 m greatly differ from the rest of distances both in frequency and in volume. This can be attributed to the differences in the frequency of large drops (exceeding 3 mm) presented in Fig. 4. In the graph presenting cumulative volume (Fig. 7.2) curves for distances 6.0, 7.5 and 9.0 appear separated and present less slope than the 1.5, 3.0 and 4.5 m curves. These groups of curves showed a more similar pattern in cumulative frequencies (Fig. 7.1).

The cumulative frequency graph shows that small drops (<2 mm of diameter) exceeded 90% frequency for distances below 10.5 m, reaching 100 % frequency (and even volume) for distances up to 4.5 m. At medium-large distances the situation changed, particularly in volume. At 6.0, 7.5 and 9.0 m the cumulative volume for small drops was 70 %, 50 % and 65 %, respectively. At the largest distances, 10.5 and at 12.5 m, the curves were less steep both in frequency and volume, indicating that the distribution of diameters was well graded. The volume of small drops (< 2 mm) was 1.5 % at 10.5 m and 0.7 % at 12.5 m.

The drop diameter range 2-5 mm was not important in terms of frequency at medium distances (4.5 to 9.0 m), averaging 5 %. However, this diameter range represented 40 % of the applied volume. Similar findings could be reported for large drops (>5 mm in diameter) at 10.5 and 12.5 m, since these drops only represented 3 % in frequency but 16 % in volume. Although frequency data are particularly interesting to analyze the validity of the ballistic model, the analysis of cumulative volume produces more insight on the significance of different drop diameter classes.

Relationships between drop diameter, velocity and angle

In the previous paragraphs relationships were described between drop diameter and the other measured variables at each observation distance (Figs. 4, 5 and 6). These descriptions were qualitative, since the variables were grouped in diameter ranges and separated by distance to the sprinkler. Figures 8 and 9 present scatter plots between drop diameter on one hand and velocity and angle on the other, for all characterized drops.

A clear trend was observed between diameter and velocity (Fig. 8), which was represented by a logarithmic model (R^2 = 0.91). This trend represents a varying proportionality. The continuous decrease in slope is related to the relationship between drop diameter and aerodynamic drag, and to the fact that small drops are observed in their final, quasi vertical trajectory, while larger drops are usually observed when their trajectory still has a relevant horizontal component. Symbols in Fig. 8 represent the observation distance, and reveal that large drops are indeed observed at distal points, while finer drops can be observed at any point, but more frequently near the nozzle.

Figure 9 presents the relationship between drop diameter and drop angle. The Figure shows an important variability in angle for small drop diameters. The trajectory of small drops was occasionally affected by turbulences distorting their vertical angle. Variability sharply decreased with drop diameter. A significant linear relationship ($p < 0.001$) could be established between both variables, although the coefficient of determination was very low. The application of the linear model to the estimation of drop angle for diameters of 0.5 and 5.0 mm resulted in angles of 80.1º and 59.1º, respectively. As a consequence, a range of 20º in drop angle should be observed in the absence of turbulences in all drop diameters and for all observation points, with the most vertical trajectories corresponding to small drops.

Volumetric analysis of drop diameter and velocity

Figure 10 presents the cumulative volume applied by each drop diameter class as a function of distance. An increase in the slope of cumulative volume lines was observed as drop diameter increased. This suggests that large drops contribute to sprinkler irrigation in a comparatively narrow circular crown. On the contrary, small drops contribute to the irrigation of wide circular crowns. 80 % of the volume applied by drops with diameter <1 mm fell between 0 and 6.0 m from the sprinkler, while 100 % fell between 0 and 9.0 m. At this last distance, drops with diameter of 1-2 mm had also applied practically all their volume. On the other hand, drops with diameter ranges 2-3 mm and 3-4 mm applied 63 % and 86 % (respectively) of their volume between 9.0 and 12.5 m to the sprinkler. Between these two distances, the largest drop class (> 4 mm) applied 100 % of their volume.

Figure 11 presents a visual representation of the results reported in Fig. 10. Drops of different diameters are depicted and located in circular crowns centred at the observation points. In this quarter-circle representation, a sample of 500 drops (and half drops) are presented and located in each circular crown following the observed frequencies. The data included in the Figure present the drop distribution in the total area irrigated by the sprinkler in terms of drop frequency and associated volume. Confirming previous results, drop density drastically decreases with distance. At the same time, drop diameter increases and compensates (in terms of volume) the decrease in density. It is interesting to note that 71.6 % of the total drops had diameters <1 mm, with a volumetric contribution of just 7.9 %. On the other hand, the largest drops (>4 mm) had a frequency of 0.7 %, but their volumetric contribution was 27.1 %.

Finally, Figure 12 presents the arithmetic (Table 1) and volume weighed average drop velocity as a function of distance to the sprinkler. The volumetric average shows an approximately linear relationship between 2 and 6 m s^{-1}, while the arithmetic average reports on a sharp increase in drop velocity between 9.0 and 10.5 m from the sprinkler.

Evaluation of the proposed photographic methodology

The proposed method permits direct, visual measurement of the drop variables. It produces quality measurements of the photographed drop population. Photographic data quality is based on the individualization of the drops and on the physical nature of the geometric determinations. Additionally, the proposed technique is low-cost, easy to setup and transport (just a camera and a screen), does not require computing power in the field and permits to measure drop angles. Finally, the proposed technique obtains three variables per drop, as compared to the diameter measurements reported in the literature for optical methods (Kincaid 1996; Montero et al. 2003).

Unfortunately, the method requires skilful operation in the field and time-consuming processing at the office. About 200 h of work were required to run the field and office phases of the reported experiments. Most of the time (about 7 min drop^{-1}) was devoted to the estimation of drop variables from the treated images. As a consequence, the proposed method results cumbersome and time consuming. Automation of this process could be addressed using image processing, although the initial programming effort could be much more intense than the reported experimentation effort.

CONCLUSIONS

The proposed technique has permitted to estimate drop diameter, velocity and angle through direct measurements, thus guaranteeing quality in the characterization of the drops present in the photographs. The photographic technique is free from some of the problems that have been described for optical methods. Diameter and velocity measurements were successfully validated, with average errors of -0.45 and 0.31 %, respectively. A certain increase in the variability of diameter and velocity was appreciated, resulting from experimental errors and from the measurement of drops located at distances up to ±0.04 m from the focus point. The proposed technique is cumbersome, just like many other direct measurement techniques reported in the literature (Sudheer and Panda 2000).

In the experimental case, results confirmed the differences in diameter, velocity and angle resulting from the distance to the sprinkler. The method permitted independent characterization of the drops emitted by the impact arm at distances of 6.0 and 7.5 m, showing relevant differences in the analysed variables with the main jet drops at the same distances. Very fine drops (<1 mm) were observed at distances of up to 9.0 m from the sprinkler, a distance where their presence can not be explained by sprinkler irrigation ballistics (Lorenzini 2004). Our findings confirm similar results by Seginer et al. (1991), Montero et al. (2003) and Burguete et al. (2007), and stress the need to reformulate ballistic theory in the sense that not all drops are formed at the nozzle. The distribution of drop velocity followed the trends reported for drop diameter, while the angle showed high variability at some distances (particularly for fine drops), which was attributed to turbulences. The volumetric frequency of drop diameters permitted to reconstruct water application along the sprinkler radius in terms of the frequency of drops of different diameters.

The reported experiment was performed at a nozzle pressure of 200 kPa, which is substantially lower than the usual nozzle pressures for this type of impact sprinklers (300-400 kPa). Finer drops should be expected at these operating pressures, which could require specific adaptations of the proposed methodology.

The proposed technique does not require specific equipment, but it is labour intensive. This methodology can provide data to run drop-by-drop simulations aiming at improving the hypotheses behind ballistic models, particularly those addressing the process of drop formation along the jet. The reported drop velocity and angle measurements will be an additional source of validation for such simulation results.

ACKNOWLEDGEMENTS

This research was funded by the Plan Nacional de I+D+i of the Government of Spain, through grant AGL2007-66716-C03. Carlos Bautista received a scholarship from the Agencia Española de Cooperación Internacional (AECI). Thanks are also due to the Universidad Autónoma de Zacatecas, México. We appreciate the technical support provided by Valero Pérez, Miguel Izquierdo and Jesús Gaudó. The order of authors in the paper follows the “first-last-author-emphasis” norm.

REFERENCES

Bedaiwy MNA (2008) Mechanical and hydraulic resistance relations in crust-topped soils. Catena 72(2): 270-281.

Burguete J, Playán E, Montero J and Zapata N (2007) Improving drop size and velocity estimates of an optical disdrometer: Implications for sprinkler irrigation simulation. Transactions of the American Society of Agricultural and Biological Engineers, 50(6), 2103-2116.

Carrión P, Tarjuelo JM, and Montero J (2001) SIRIAS: a simulation model for sprinkler irrigation: I. Description of the model. Irrigation Science, 2001(20), 73-84.

Cruvinel PE, Minatel ER, Mucheroni ML, Vieira SR and Crestana S (1996) An Automatic Method Based on Image Processing for Measurements of Drop Size Distribution from Agricultural Sprinklers. Anais do IX SIBIGRAPI, 39-46.

Cruvinel PE, Vieira SR, Crestana S, Minatel R, Mucheroni ML and Neto AT (1999) Image processing in automated measurements of raindrop size and distribution. Computers and Electronics in Agriculture, 23(3), 205-217.

De Lima JLMP and Torf PJJF (1994) Effects of wind on simulated rainfall and overland flow under single full-cone nozzle sprays. Proceedings of the Second European Conference on Advances in Water Resources Technology and Management. pp. 443–450, In: Trakiris, G. and Santos, M.A., Editors,, Balkema, Lisbon, Portugal.

De Lima JLMP, Torfs PJJF and Singh VP (2002) A mathematical model for evaluating the effect of wind on downward-spraying rainfall simulators. Catena, 46(4), 221-241.

Edling RJ (1985) Kinetic energy, evaporation and wind drift of droplets from low pressure irrigation nozzles. Transactions of the American Society of Agricultural Engineers 28(5): 1543-1550.

Eigel JD and ID Moore (1983) A simplified technique for measuring raindrop size and distribution. Transactions of the American Society of Agricultural Engineers 26(4): 1079-1084.

Fukui Y, Nakanishi K and Okamura S (1980) Computer evaluation of sprinkler irrigation uniformity. Irrigation Science, 2, 23-32.

Hauser D, Amayenc P, Nutten B and Waldteufel P (1984) A new optical instrument for simultaneous measurement of raindrop diameter and fall speed distributions. Journal of Atmospheric and Oceanic Technology, 1(3), 256-269.

Jones DMA (1956) Rainfall drop-size distribution and radar reflectivity. Rainfall Drop-size. Distribution and Radar Reflectivity: 20.

Joss J and Waldvogel A (1967) Ein Spectrograph für Niederschlagstropfen mit automatisher Auswertung (A spectrograph for the automatic analysis of raindrops). Pure and Applied Geophysics. 68: 240–246.

Keller J and Bliesner RD (1990) Sprinkle and trickle irrigation. New York, NY, Van Nostrand Reinhold.

Kincaid DC (1996) Spraydrop kinetic energy from irrigation sprinklers. Transactions of the American Society of Agricultural Engineers 39(3): 847-853.

Kincaid DC, Solomon KH and Oliphant JC (1996) Drop size distributions for irrigation sprinklers. Transactions of the American Society of Agricultural Engineers, 39(3), 839-845.

Kohl RA and DeBoer DW (1984) Drop size distributions for a low pressure spray type agricultural sprinkler. Transactions of the American Society of Agricultural Engineers 27(6): 1836-1840.

Lorenzini G (2004) Simplified modelling of sprinkler droplet dynamics. Biosystems Engineering 87(1): 1-11.

Lorenzini G (2006) Water droplet dynamics and evaporation in an irrigation spray. Transactions of the ASABE, 49(2), 545-549.

Magarvey RH (1956) Stain Method of drop size determination. Journal of Meteorology 14: 182-184.

Montero J, Tarjuelo JM and Carrión P (2001) SIRIAS: a simulation model for sprinkler irrigation: II. Calibration and validation of the model. Irrigation Science, 2001(20), 85-98.

Montero J, Tarjuelo JM and Carrión P (2003) Sprinkler droplet size distribution measured with an optical spectropluviometer. Irrigation Science, 2003(22), 47-56.

Playán E, Salvador R, Faci JM, Zapata N, Martínez-Cob A and Sánchez I (2005) Day and night wind drift and evaporation losses in sprinkler solid-sets and moving laterals. Agricultural Water Management, 76(3), 139-159.

Playán E, Zapata N, Faci JM, Tolosa D, Lacueva JL, Pelegrín J, Salvador R, Sánchez, I and Lafita A (2006) Assessing sprinkler irrigation uniformity using a ballistic simulation model." Agricultural Water Management, 84(1-2), 89-100.

Salles C, Poesen J and Borselli L (1999) Measurement of simulated drop size distribution with an optical spectro-pluviometer: Sample size considerations. Earth Surface Processes and Landforms, 24(6), 545-556.

Seginer I, Nir D and von Bernuth D (1991) Simulation of wind-distorted sprinkler patterns. Journal of Irrigation and Drainage Engineering, ASCE, 117(2), 285-306.

Sudheer KP and Panda RK (2000). Digital image processing for determining drop sizes from irrigation spray nozzles. Agricultural Water Management 45(2000): 159-167.

Tarjuelo, JM, Ortega JF, Montero J and De Juan JA (2000) Modelling evaporation and drift losses in irrigation with medium size impact sprinklers under semi-arid conditions. Agricultural Water Management, 43(2000), 263-284.

Thompson AL, Gilley JR and Norman JM (1986) Simulation of sprinkler water droplet evaporation above a plant canopy. Paper - American Society of Agricultural Engineers.

Trimer WL (1987) Sprinkler evaporation loss equation. Journal of Irrigation and Drainage Engineering, ASCE 113(4): 616-620.

Von Bernuth RD and Gilley JR (1984) Sprinkler droplet size distribution estimation from single leg test data. Transactions of the American Society of Agricultural Engineers, 27(5), 1435-1441.

Wiesner J (1895) Beiträge zur Kentniss der Grösze des tropischen Regens. Akademie der Wissenschaften, Mathematika-Naturwissenschaften Klasse, vol. 104, Sitz Berlin Verlag, pp. 1397–1434.

LIST OF TABLES

LIST OF FIGURES

Figure 10. Cumulative volume applied by each drop diameter class as a function of distance to the nozzle. Data are presented for different drop diameter classes.

Figure 11. Representation of drop distribution resulting from the experimental sprinkler in a quarter-circle. A total of 500 drops (and half drops) are distributed at different distances from the nozzle.

Figure 12. Arithmetic and volume weighed average drop velocity as a function of distance to the sprinkler.

Table 1

Distance (m)	***Number of Drops***	***Diameter (mm)***			***Velocity (m s^{-1})***			***Angle (º)***		
		Average	***Min***	***Max***	***Average***	***Min***	***Max***	***Average***	***Min***	***Max***
1.5	354	0.6	0.4	1.6	1.9	1.0	3.8	94	65	105
3.0	205	0.7	0.5	1.6	2.4	1.4	3.6	70	53	84
4.5	135	0.8	0.3	1.8	2.5	0.9	4.1	75	39	112
6.0	260	0.9	0.4	2.5	2.5	0.9	5.2	67	43	98
7.5	156	1.1	0.4	3.8	3.1	0.9	5.9	88	60	107
9.0	184	1.1	0.4	3.1	3.3	1.0	6.3	67	51	86
10.5	109	3.0	1.3	6.8	5.6	4.2	7.5	73	61	87
12.5	61	3.3	1.7	6.4	5.5	4.2	7.2	69	60	79

Fig. 1

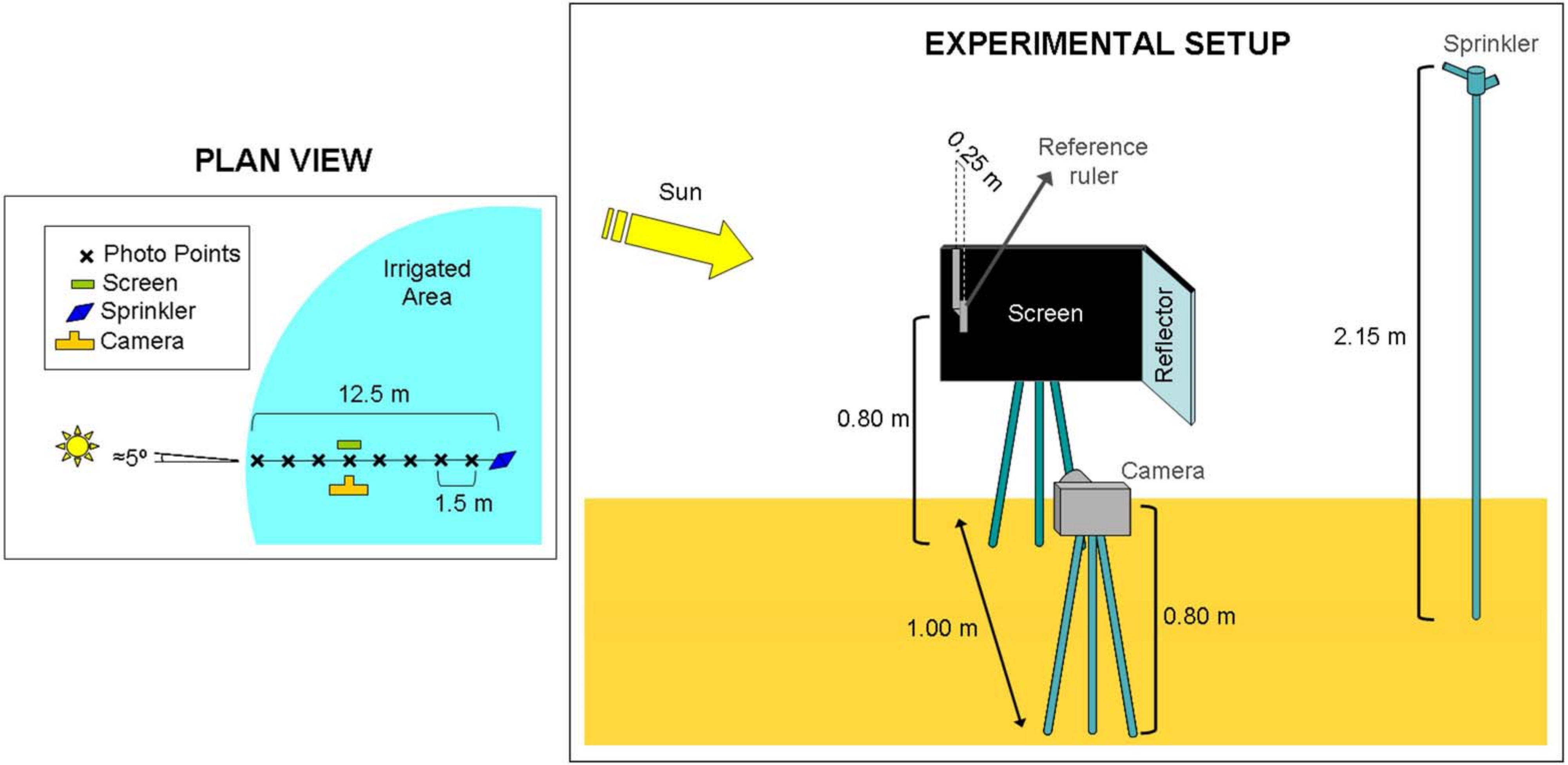

PLAN VIEW
Photo Points
Screen
Sprinkler
Camera
Irrigated Area
12.5 m
≈5º
1.5 m
EXPERIMENTAL SETUP
Sprinkler
Sun
0.25 m
Reference ruler
Screen
Reflector
2.15 m
0.80 m
Camera
1.00 m
0.80 m

Fig. 2

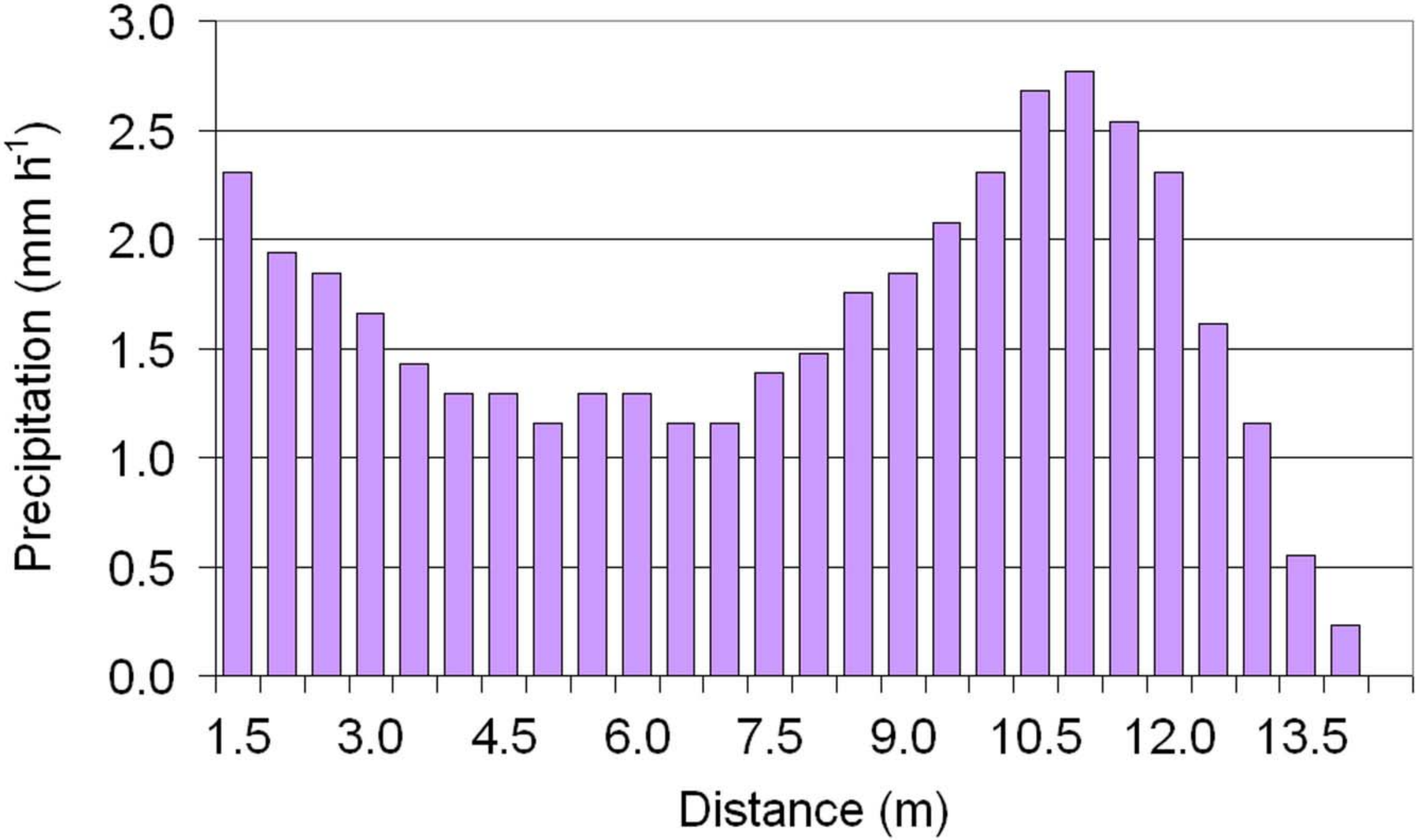

Precipitation (mm h-1)
3.0
2.5
2.0
1.5
1.0
0.5
0.0
1.5
3.0
4.5
6.0
7.5
9.0
10.5
12.0
13.5
Distance (m)

Fig. 3

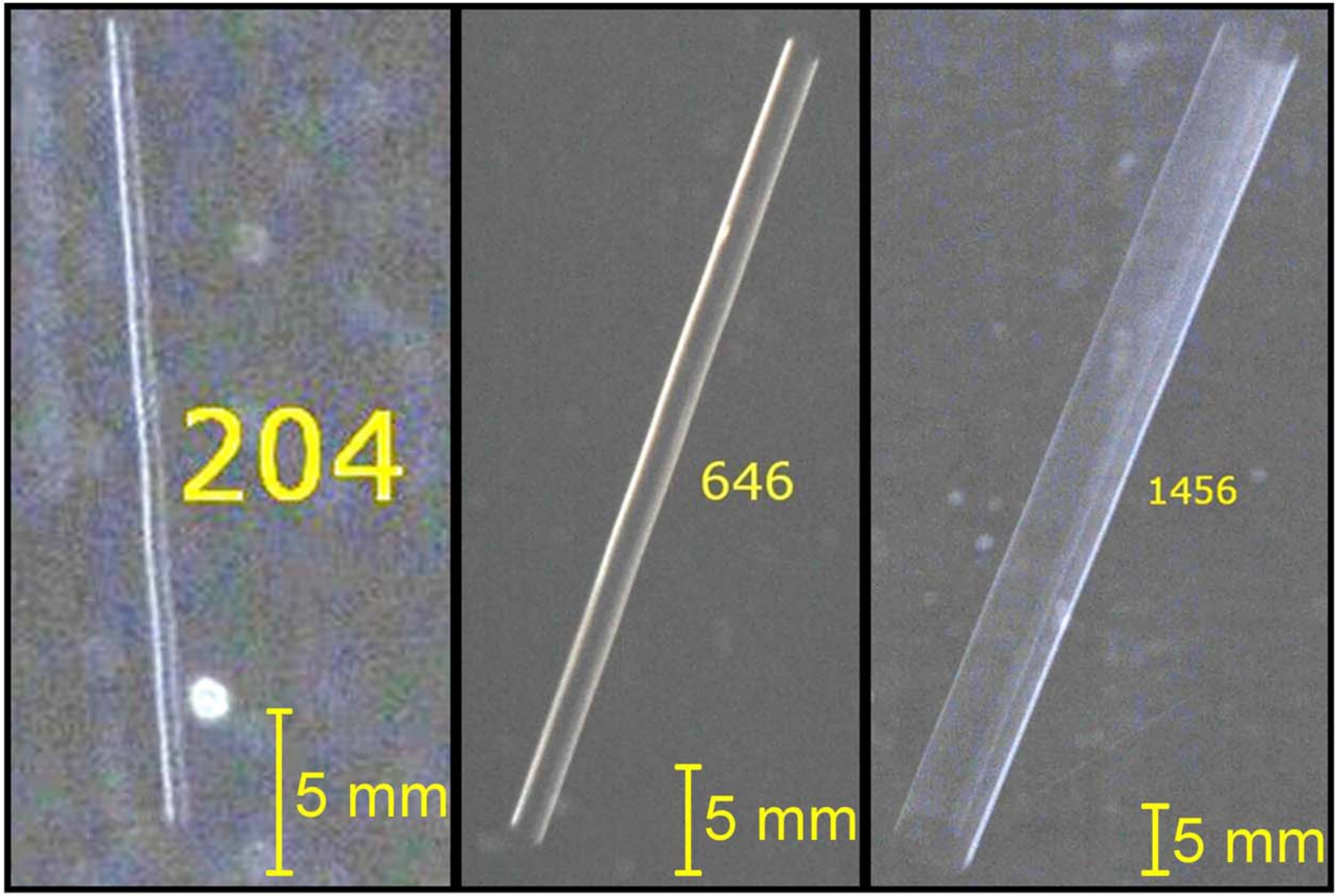

D = 1.5 m
∅ = 0.66 mm
V = 1.9 m/s
â = 94°

D = 4.5 m
∅ = 1.84 mm
V = 4.1 m/s
â = 71°

D = 12.5 m
∅ = 6.36 mm
V = 6.4 m/s
â = 68°

Fig. 4

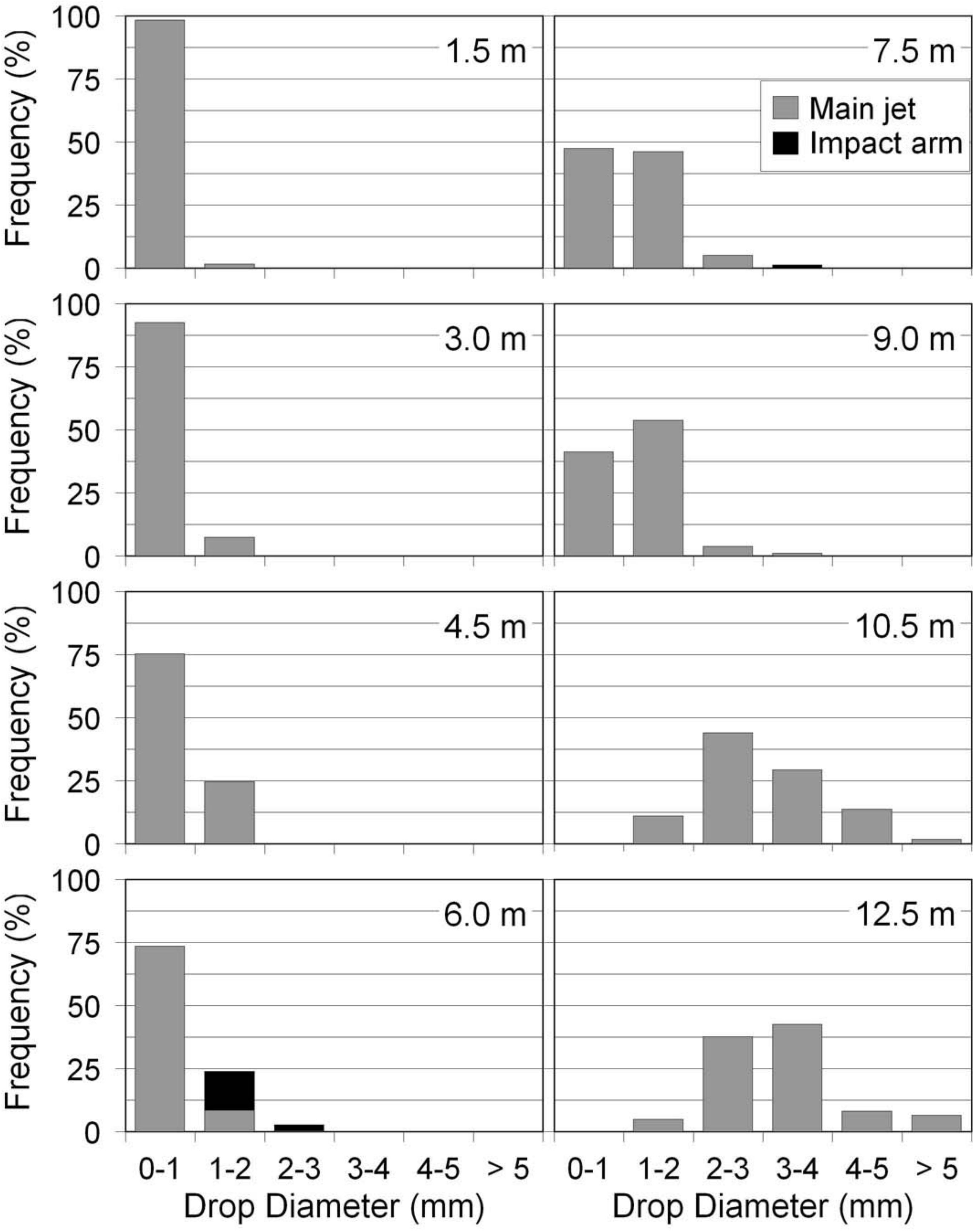

Frequency (%)
100
75
50
25
0
1.5 m
7.5 m
Main jet
Impact arm
3.0 m
9.0 m
4.5 m
10.5 m
6.0 m
12.5 m
0-1
1-2
2-3
3-4
4-5
> 5
Drop Diameter (mm)

Fig. 5

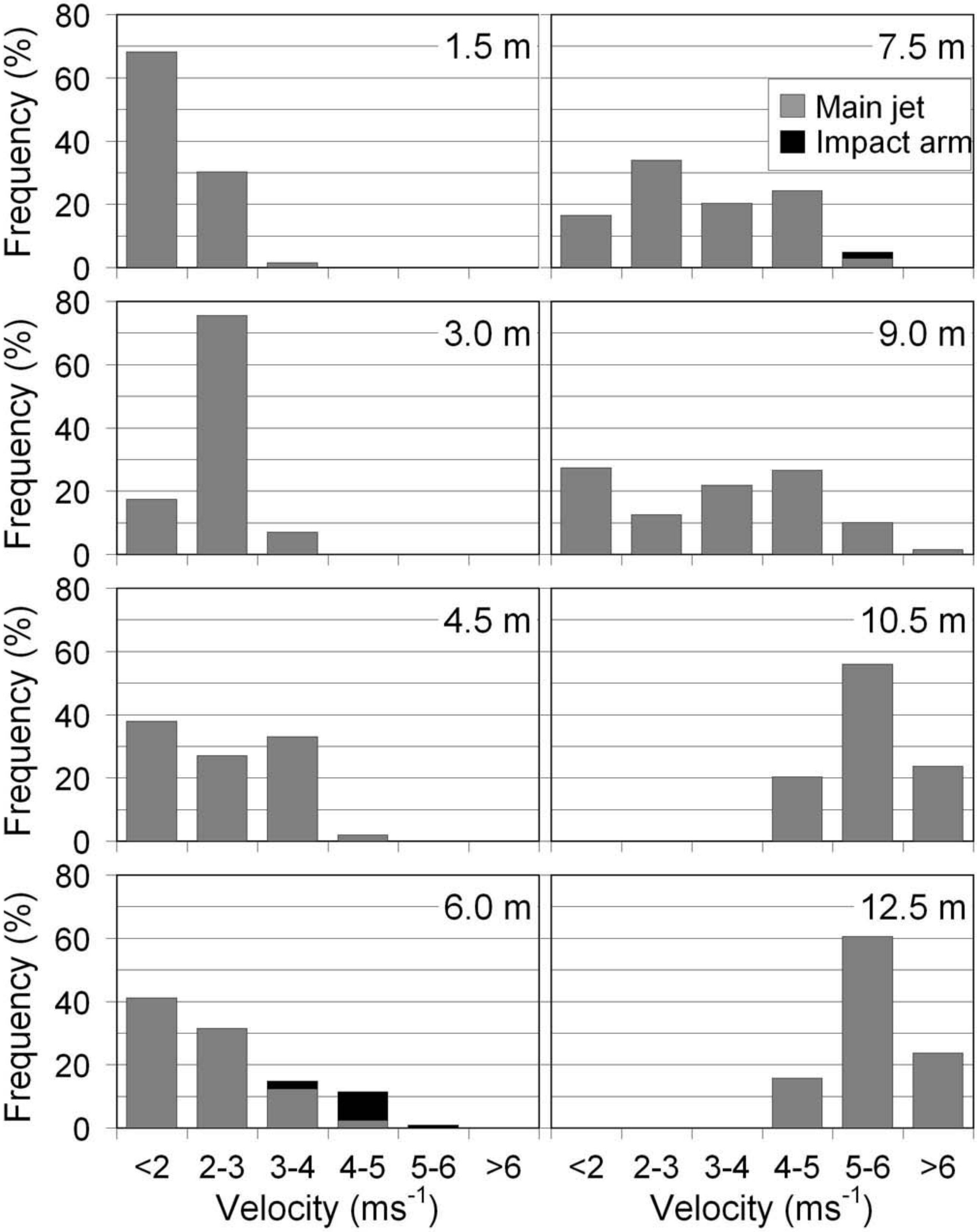

1.5 m
7.5 m
3.0 m
9.0 m
4.5 m
10.5 m
6.0 m
12.5 m
Main jet
Impact arm
Frequency (%)
0
20
40
60
80
<2
2-3
3-4
4-5
5-6
>6
Velocity (ms-1)

Fig. 6

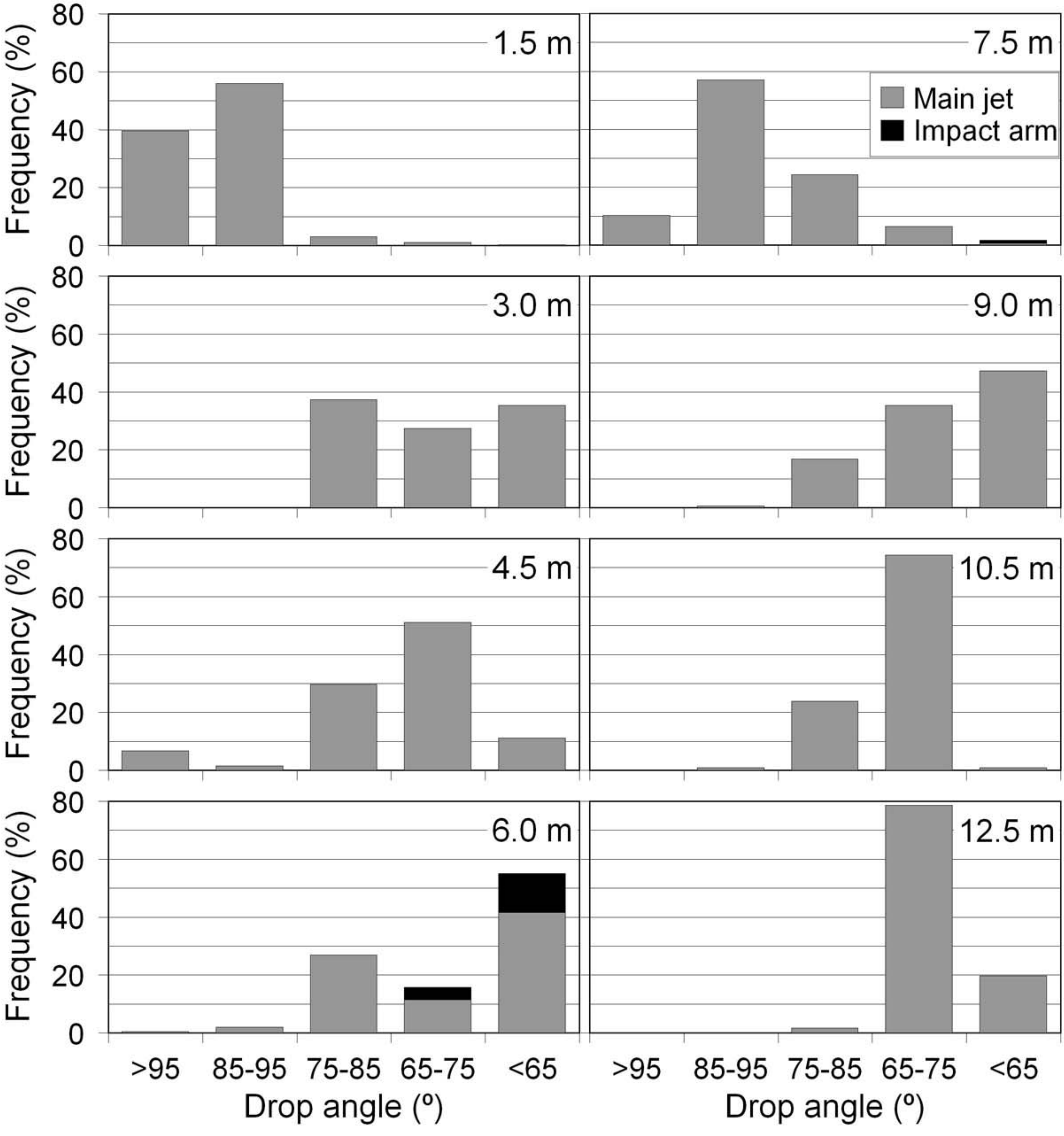

1.5 m
7.5 m
Main jet
Impact arm
3.0 m
9.0 m
4.5 m
10.5 m
6.0 m
12.5 m
Frequency (%)
80
60
40
20
0
>95
85-95
75-85
65-75
<65
Drop angle (º)

Fig. 7

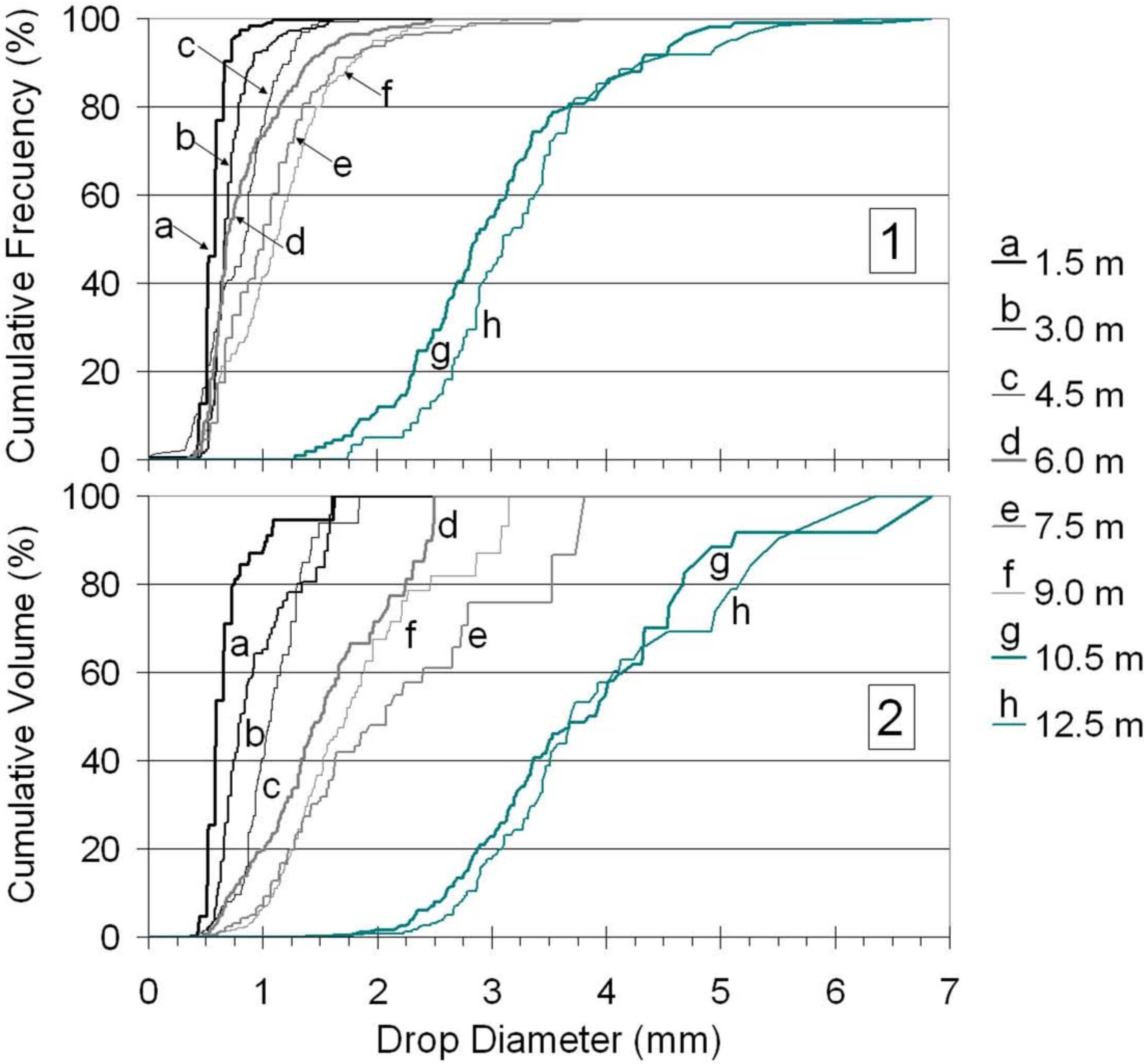

Cumulative Frecuency (%)
100
80
60
40
20
0
c
b
a
d
e
f
g
h
1
Cumulative Volume (%)
100
80
60
40
20
0
a
b
c
d
f
e
g
h
2
0
1
2
3
4
5
6
7
Drop Diameter (mm)
a 1.5 m
b 3.0 m
c 4.5 m
d 6.0 m
e 7.5 m
f 9.0 m
g 10.5 m
h 12.5 m

Fig. 8

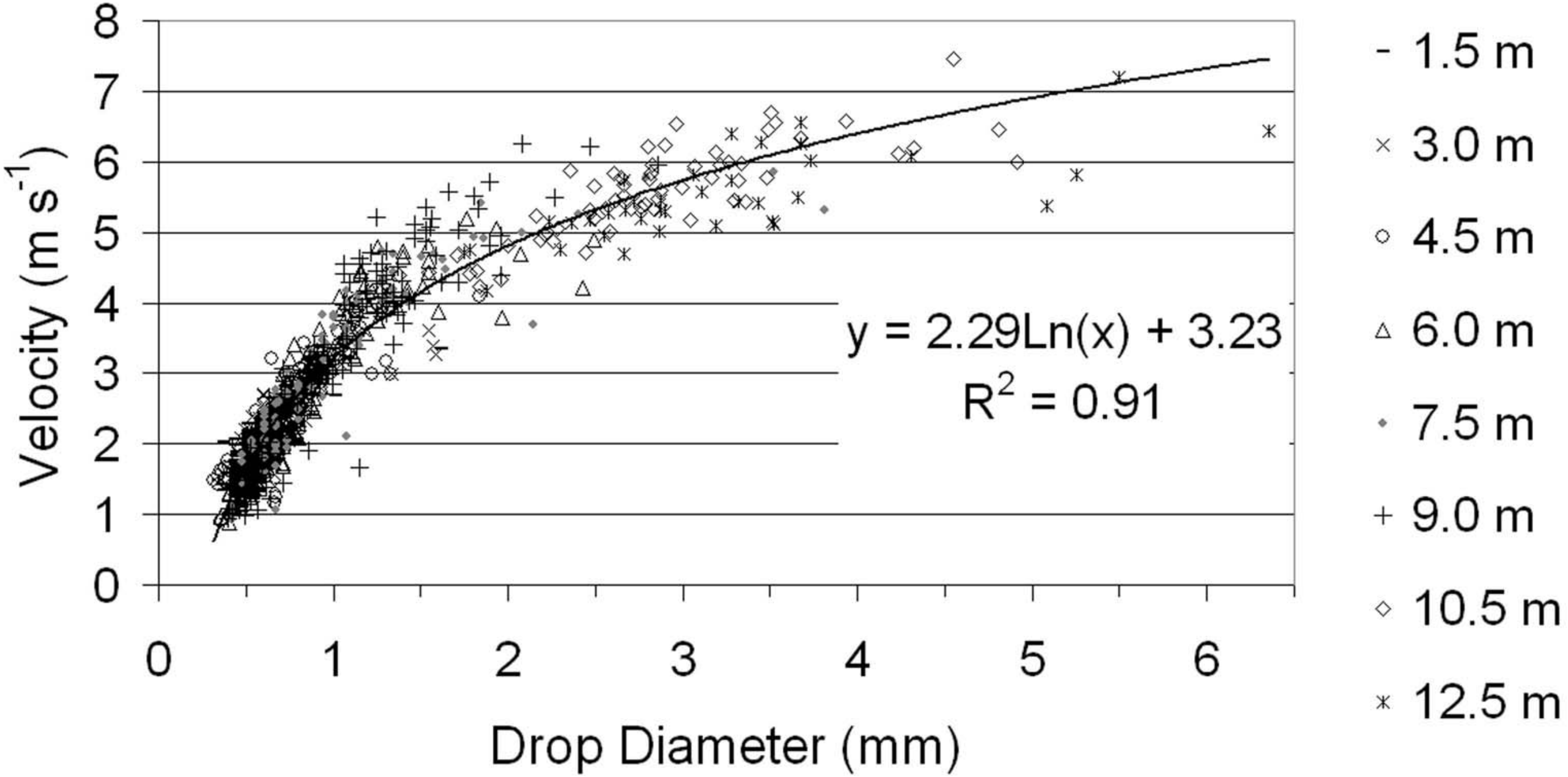

8
7
6
5
4
3
2
1
0
Velocity (m s-1)
0
1
2
3
4
5
6
Drop Diameter (mm)
y = 2.29Ln(x) + 3.23
R2 = 0.91
1.5 m
3.0 m
4.5 m
6.0 m
7.5 m
9.0 m
10.5 m
12.5 m

Fig. 9

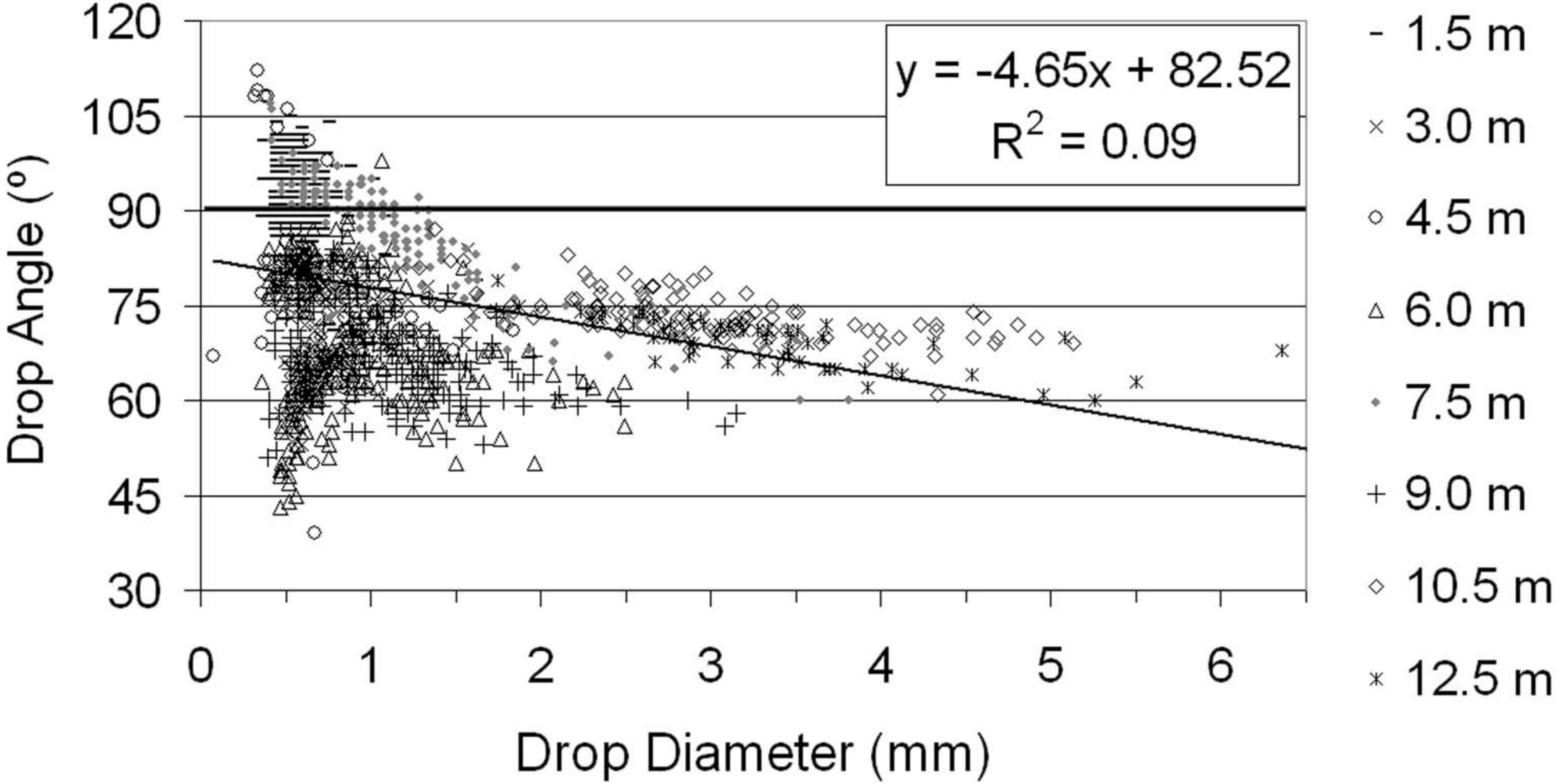

y = -4.65x + 82.52
R2 = 0.09
Drop Angle (º)
Drop Diameter (mm)
120
105
90
75
60
45
30
0
1
2
3
4
5
6
- 1.5 m
× 3.0 m
○ 4.5 m
△ 6.0 m
◆ 7.5 m
+ 9.0 m
◇ 10.5 m
✳ 12.5 m

Fig. 10

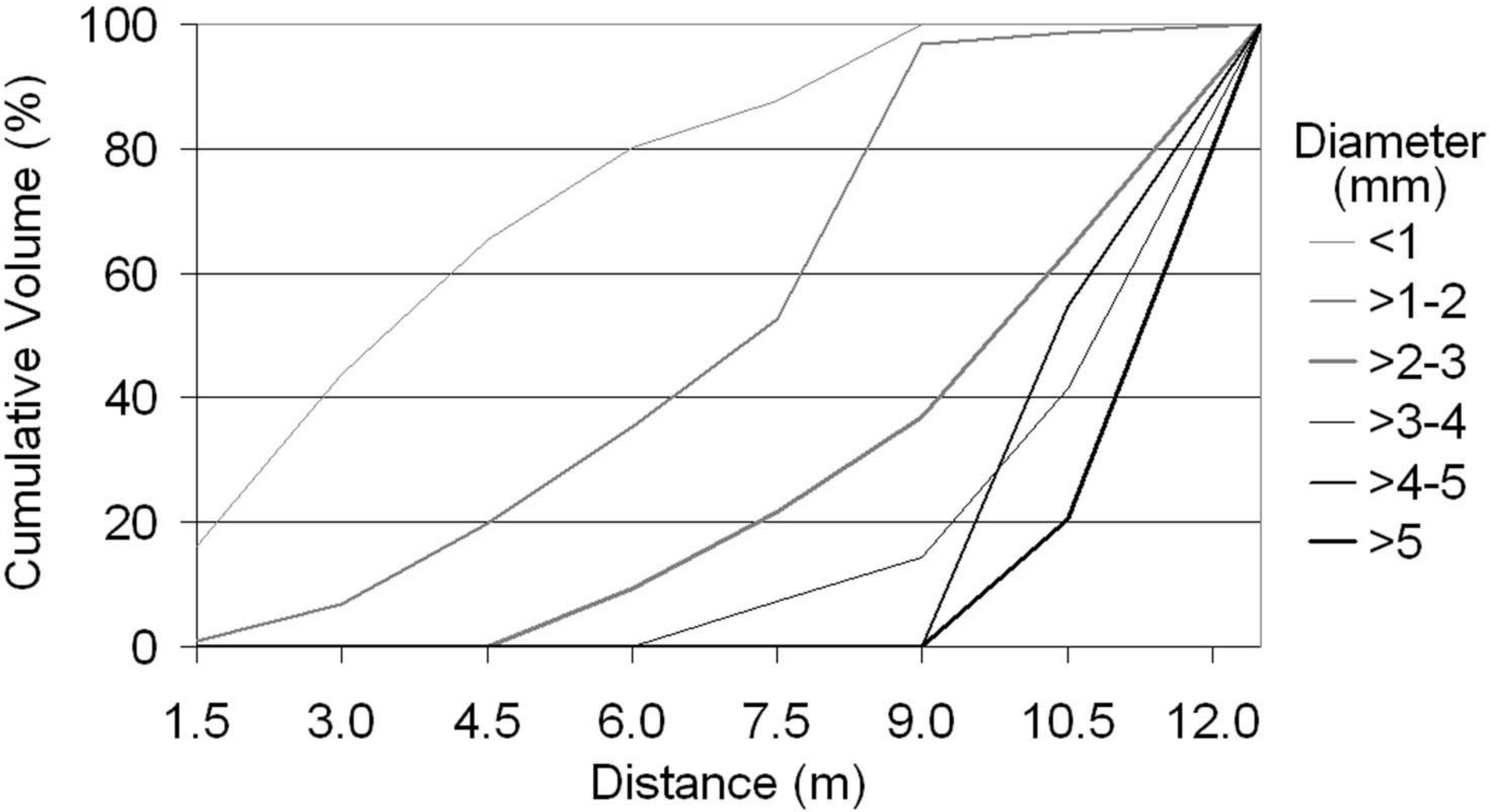

100
80
60
40
20
0
Cumulative Volume (%)
1.5
3.0
4.5
6.0
7.5
9.0
10.5
12.0
Distance (m)
Diameter (mm)
<1
>1-2
>2-3
>3-4
>4-5
>5

Fig. 11

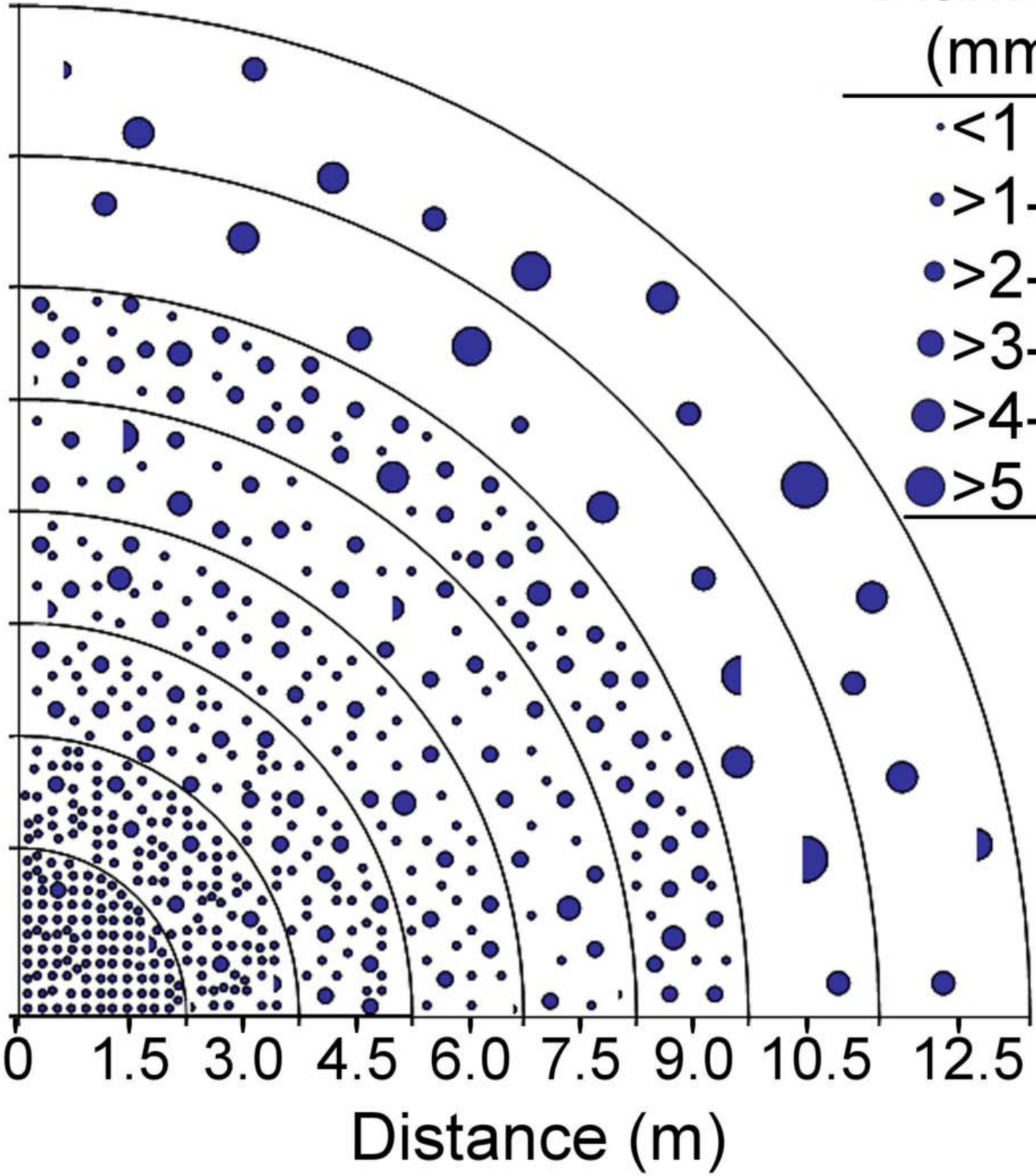

Diameter (mm)	Frequency (%)	Volume (%)
<1	71.6	7.9
>1-2	22.5	19.6
>2-3	3.3	18.4
>3-4	1.9	27.0
>4-5	0.5	14.1
>5	0.2	13.0

Fig. 12

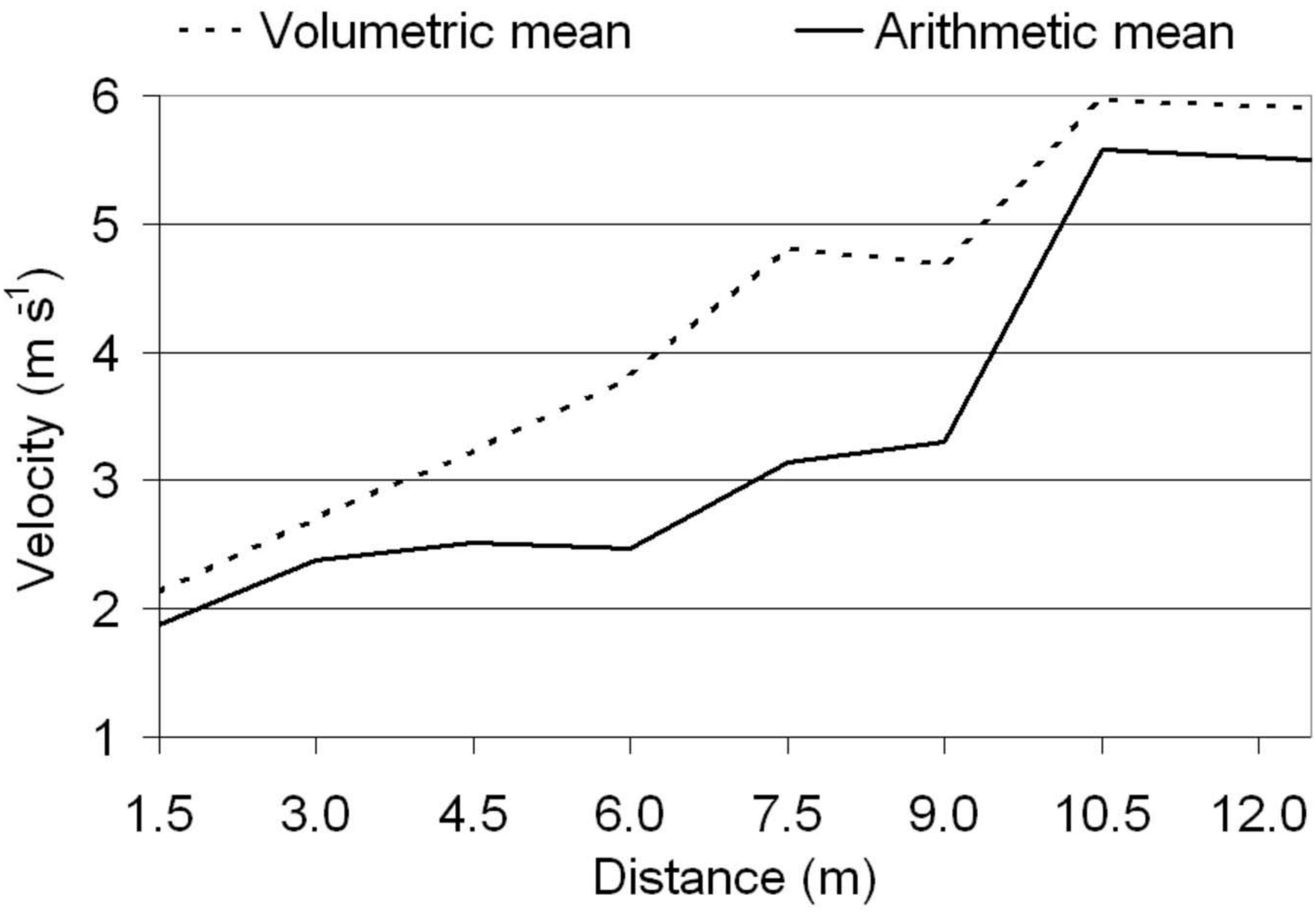

Volumetric mean
Arithmetic mean
6
5
4
3
2
1
Velocity (m s-1)
1.5
3.0
4.5
6.0
7.5
9.0
10.5
12.0
Distance (m)